2025 IEEE 53rd Photovoltaic Specialists Conference (PVSC) | 979-8-3315-3444-8/25/$31.00 ©2025 IEEE | DOI: 10.1109/PVSC59419.2025.11133345

Colloidal-Quantum-Dot Enhanced Photovoltaic Responses of GaAs Solar Cells with Atomic Layer Deposition Passivation Layer

Chin-I Chen[1], Tao Deng[1], Kai-Ling Liang[2], Wei-Hung Kuo[2], Bo-Ming Huang[1], Yu-Ting Hsieh[1], JyunWei Ji[3], SungYu Chen[3], Chien-Chung Lin[1]

[1]Graduate Institute of Photonics and Optoelectronics, National Taiwan University, Taipei 106, Taiwan
[2]Electronic and Optoelectronic System Research Laboratories, Industrial Technology Research Institute, Chutung, Hsinchu 310, Taiwan
[3]Advanced Photovoltaic and System Application Division, Green Energy and Environment Research Laboratories, Industrial Technology Research Institute, Tainan 711, Taiwan

***Abstract* — In this study, a novel mesa design of GaAs single junction solar cells were implemented with a passivation layer deposited by an atomic layer deposition (ALD) system. With the addition of a colloidal quantum dot layer to enable the luminescent downshifting effect, we are able to demonstrate an enhancement of the short-circuit current density as high as 33.75%. The power conversion efficiency of such devices can also be increased by 22.37% in the best case. Further analysis showed the nearly size-independent dark current density among various ALD-passivated devices.**

I. Introduction

In the advances of artificial intelligence (AI), the power-demanding data centers have become a necessity in each network architecture. With looming high power consumption, a green energy strategy will be needed to curb down the energy we spent to transmit data. Among all the current technologies, semiconductor-based solar cells have been treated as the major player for the future development. While the power conversion efficiency (PCE) of such devices has improved a lot in the past decades [1], incremental enhancements are still much welcomed because of the eventual cost-saving in the long-term operation. In order to achieve this, researchers have shown several prominent methods: tandem cell designs, heterogeneous integration of different materials (such as perovskite and Si [2]), optical designs (such as luminescent solar concentrators [3]). These designs helped to promote the semiconductor based photovoltaic devices to one of the most successful green technologies today. One of the potential solutions to further improve the PCE should be the incorporation of the novel photonic materials, such as colloidal quantum dots (CQDs) [4-6], which can provide high quantum yields, and their capability to be photon-sensitive is quite remarkable. Although it is not an easy job to have an electrically driven photonic devices out of these CQDs, an heterogeneously integrated scheme is potentially viable by utilizing the luminescent downshifting (LDS) effect [7]. To incorporate LDS effect, one might need to re-assess the device layout design which might place different influences on the CQD-induced carrier generation. In our earlier study, we reported enhancement of a series of photovoltaic devices by placing the CQD layers inside the device [4, 7]. In this paper, we will reveal our latest progress in this direction and further analyze the results by different passivation layers of the devices' sidewalls. As one might feel interested, the passivation of the sidewalls can directly affect the dark current density of the devices and thus the fill factor and the open-circuit voltage accordingly. Our devices possess mesa with various different shapes, which could greatly change the traditional thinking of square or circular shape mesas.

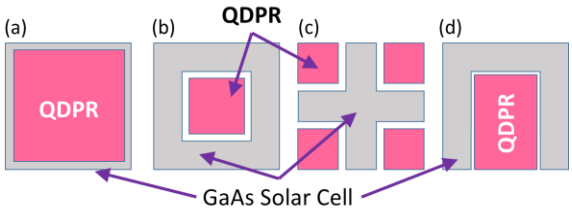

Fig. 1. The device and CQD layer layouts for (a)square; (b)hollowed square; (c)cross-shape; (d)U-shape.

II. Experimental Setup

In this section, we will discuss our fabrication processes and steps of integration. The wafers were purchased from the external vendors (Visual Photonics Epitaxy Co. Ltd., Taiwan). The epitaxial structure is a single junction GaAs-based pn photodiode with a reduced doping region for the main photon-absorption section. The wafer would go through the regular cleaning process and the photolithography steps to be patterned into different shapes of mesas. The mesa can be dry-etched by an inductively coupled plasma (ICP) system with the mixed BCl_3, Cl_2, and Ar gases and the etch depth is 1.4 μm. After dry-etch, two different types of passivation measures were taken: (a) a 44nm atomic layer deposited (ALD) Al_2O_3 and a 44nm PECVD SiO_2 layer; (b) an 88nm PECVD SiO2 layer. The choice of dielectric thickness corresponds to the potential anti-reflection (AR) coating effect we need for the maximum reception of solar energy for each device. Four different shapes were carried out in this set of experiments: square, hollowed square, cross-shape and U-shape, as shown in Fig. 1. The CQD layer were formed by quantum-dot-photoresist (QDPR). The active material of CQD is CdSe/ZnS core-shell structure purchased from Unique Materials Co., Taiwan. The photoresist was purchased from Advanced Echem Materials Company Limited, Taiwan. The detailed process steps to pattern the QDPR can be found in our previous work [8], and the corresponding location of each QDPR pattern can also be seen

in Fig. 1. After the devices were fabricated, the normal photovoltaic properties were firstly measured and recorded. The short-circuit current (I_{sc}), the open-circuit voltage (V_{oc}), and the fill factor, the external quantum efficiency (EQE) were all recorded in order to make the comparison later.

III. Results and Discussions

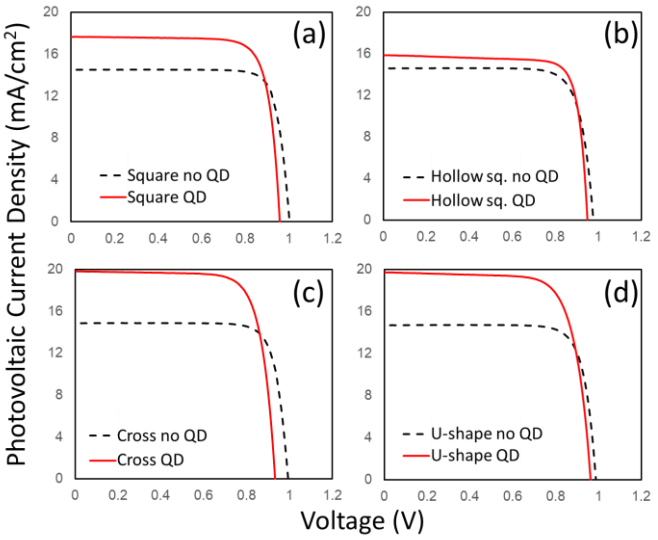

Fig. 2. Example of readable plot using different colors and line styles for clarity.

TABLE I
SUMMARY OF PHOTOVOLTAIC CHARACTERISTICS OF NOVEL SOLAR CELLS WITH AND WITHOUT CQD LAYERS

Type of mesa/ CQD	Square		Hollowed Square		Cross		U-shape	
	No QD	QD	No QD	QD	No QD	QD	No QD	QD
V_{oc} (V)	1.00	0.96	0.98	0.95	0.99	0.93	0.99	0.96
J_{sc} (mA/cm^2)	14.48	17.59	14.53	15.67	14.77	19.70	14.66	19.61
PCE(%)	11.98	13.48	11.29	12.17	11.91	14.20	11.63	14.23

Fig. 2 shows our photovoltaic J-V characteristics among various shapes of devices and Table I shows the detailed numbers of the device's photovoltaic characteristics. The increased J_{sc} can be observed when CQD layers were put down to the devices and as high as 33.75 % of increase can be recorded. One important feature that we need to address is the maintenance of the V_{oc} after the CQD deployment. Because the material can generate electron-hole pairs after the light excitation, which was observed before [7], it is always a concern whether this CQD layer will affect the device electronically. We can prevent this from happening if proper isolation layer, which is the SiO_2 layer in our case, was deposited beforehand. All the devices kept high V_{oc} (>0.9 Volts) in this study and the fill factors varied between 0.75 and 0.82, which can be further improved by reducing shunt resistance of the devices. Meanwhile, the power conversion efficiencies (PCEs) of the devices with CQD layers also experienced great enhancement. As high as 22.37 % of PCE increase can be seen in the U-shape devices between CQD and non-CQD samples.

The reverse current density is a good indicator of a diode whether any leakage path exists inside the device. With the device's large mesa, certain defects in bulk region and in the peripheral (i.e. the sidewalls) region can both contribute to this reverse current density. Therefore, this current density could then be expressed as the following formula [9-11]:

$$J_0 = J_b + \frac{P}{A} \times J_p \quad (1)$$

, where J_b and J_p are the bulk and peripheral saturation current density, respectively. When we plot this J_0 against the P/A ratio, we would expect certain tendency developed among different sizes of devices. In Fig. 3, we put together the PECVD- and ALD-coated device's results and saw very different J_p. In Eq. (1), the P/A ratio can be used as the variable and then the slope of the J_0 vs. P/A ratio can be viewed as J_p, while the bulk current density J_b is the intercept from the linear regression of the data. The fitted numerical J_p is 3.54×10^{-8} A/cm for the PECVD case, while J_p becomes 3.97×10^{-9} A/cm for the ALD case. A ten-times reduction in the peripheral recombination current can be deduced from this experiment. At the same time, the Jb values for PECVD- and ALD-coated samples are 2.29×10^{-6} A/cm2 and 2.16×10^{-6} A/cm2, respectively. The similar Jb values in both cases indicate that both chips shared the similar bulk condition, as we expected.

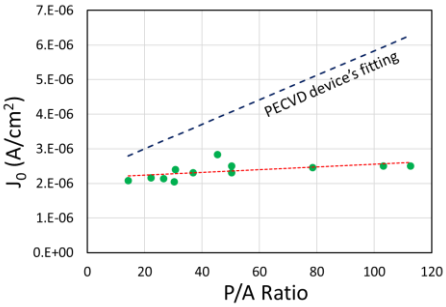

Fig. 3. The reverse biased diode current measured in the ALD devices (in green symbols). The blue dashed lines are the linear fitting of the PECVD's cases.

Another analysis can be made in the EQE spectrum. If we divided the CQD-embedded EQE by the no-CQD EQE, we will get the results in Fig. 4. The extraordinary enhancement in efficiency can be observed, and we also marked a baseline (dashed) which could be the divide between the AR effect and the LDS effect [12]. As we could expect, the AR effect becomes more dominant at longer wavelength range (such as λ>650nm, when the CQD stops absorbing and becomes completely refractive.) Meanwhile, we believe that the optical coating on our sample should be further improved because the AR effect can be as high as 5 times and this number is quite large compared to our previous study[12]. Further analysis will be needed by characterizing the surface reflectivity to clarify the AR effect and to exclude it from the LDS effect completely. The reason why we saw such a high multiplication of EQE or

J_{sc} in the CQD-coated devices could be attributed to the design of our QDPR patterns. The QDPR pattern does not overlap with the semiconductor mesa of the non-traditional device and this situation can help to collect extra solar photons from the CQD layer while the semiconductor solar cell itself was affected very little. Therefore, any CQD photons, which are generated by solar photons from the LDS effect, can be viewed as the addition to the original photovoltaic response.

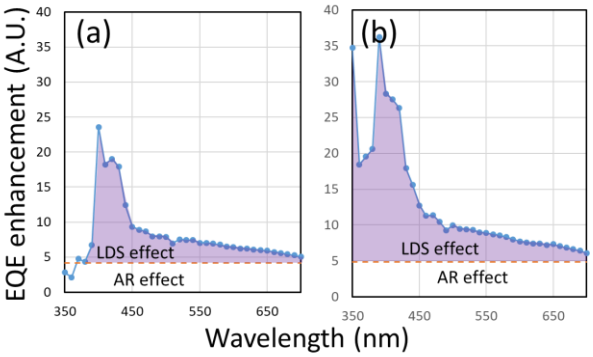

Fig. 4. The EQE enhancement of (a) a square device and (b) a U-shape device.

IV. Conclusion

In summary, we demonstrated a detailed study targeting to utilize the LDS effect in the CQD color conversion layer. The layout of the device and the CQD layer are designed to alleviate the potential heat generation issue that could be harmful for the CQD material's long-term performance. The current results showed significant enhancement in both the EQE and the short-circuit current density in the photovoltaic measurement. This encouraging result by combining the ALD passivation and the CQD LDS layer can lead us to the next generation of the semiconductor based solar cells.

References

[1] M. A. Green *et al.*, "Solar cell efficiency tables (Version 63)," *Progress in Photovoltaics: Research and Applications,* vol. 32, no. 1, pp. 3-13, 2024, doi: https://doi.org/10.1002/pip.3750.

[2] E. Aydin *et al.*, "Pathways toward commercial perovskite/silicon tandem photovoltaics," *Science,* vol. 383, no. 6679, p. eadh3849, 2024, doi: doi:10.1126/science.adh3849.

[3] V. I. Klimov, T. A. Baker, J. Lim, K. A. Velizhanin, and H. McDaniel, "Quality Factor of Luminescent Solar Concentrators and Practical Concentration Limits Attainable with Semiconductor Quantum Dots," *ACS Photonics,* vol. 3, no. 6, pp. 1138-1148, 2016/06/15 2016, doi: 10.1021/acsphotonics.6b00307.

[4] H.-C. Chen *et al.*, "Enhanced efficiency for c-Si solar cell with nanopillar array via quantum dots layers," *Optics Express,* vol. 19, no. S5, pp. A1141-A1147, 2011/09/12 2011, doi: 10.1364/OE.19.0A1141.

[5] S. Hsu, Y. Huang, Y. Kao, H. Kuo, R. Horng, and C. Lin, "The Analysis of Dual-Junction Tandem Solar Cells Enhanced by Surface Dispensed Quantum Dots," *IEEE Photonics Journal,* vol. 10, no. 5, pp. 1-11, 2018, doi: 10.1109/JPHOT.2018.2865538.

[6] K.-L. Liang *et al.*, "Highly Efficient Fine-Pitch Quantum Dot/Titanium Oxide Nanocomposites for Ultrahigh-Resolution Full-Color Micro-Light Emitting Diode Displays," *ACS Photonics,* vol. 11, no. 8, pp. 2981-2991, 2024/08/21 2024, doi: 10.1021/acsphotonics.4c00027.

[7] C.-C. Lin *et al.*, "Highly efficient CdS-quantum-dot-sensitized GaAs solar cells," *Optics Express,* vol. 20, no. S2, pp. A319-A326, 2012/03/12 2012, doi: 10.1364/OE.20.00A319.

[8] C.-C. Lin *et al.*, "Fabricating Quantum Dot Color Conversion Layers for Micro-LED-Based Augmented Reality Displays," *ACS Applied Optical Materials,* vol. 2, no. 7, pp. 1303–1313, 2023/08/02 2023, doi: 10.1021/acsaom.3c00104.

[9] A. Belghachi and S. Khelifi, "Modelling of the perimeter recombination effect in GaAs-based micro-solar cell," *Sol. Energy Mater. Sol. Cells,* vol. 90, no. 1, pp. 1-14, 2006/01/06/ 2006, doi: https://doi.org/10.1016/j.solmat.2005.01.009.

[10] T. B. Stellwag, M. R. Melloch, M. S. Lundstrom, M. S. Carpenter, and R. F. Pierret, "Orientation - dependent perimeter recombination in GaAs diodes," *Applied Physics Letters,* vol. 56, no. 17, pp. 1658-1660, 1990, doi: 10.1063/1.103108.

[11] C.-I. Chen, T. Deng, K.-L. Liang, W.-H. Kuo, and C.-C. Lin, "Strong Efficiency Enhancement of GaAs Solar cells with Quantum Dot Photoresist," presented at the 53rd IEEE Photovoltaic Specialists Conference (PVSC 53) (accepted), Montreal, Canada, 2025.

[12] H.-V. Han *et al.*, "A Highly Efficient Hybrid GaAs Solar Cell Based on Colloidal-Quantum-Dot-Sensitization," *Sci. Rep.,* Article vol. 4, p. 5734 07/18/online 2014, doi: 10.1038/srep05734.